Empirical mode with a variable spatial-temporal structure and the dynamics of superradiant lasers

E R Kocharovskaya[1], A S Gavrilov[1], V V Kocharovsky[1,2], E M Loskutov[1], D N Mukhin[1] A M Feigin[1] and Vl V Kocharovsky[1]

[1]Institute of Applied Physics of the RAS, 603950, Nizhny Novgorod, Russia
[2]Department of Physics and Astronomy, Texas A&M University, College Station, TX, USA

E-mail: kochar@appl.sci-nnov.ru

Abstract. An approach of the empirical modes with a variable spatial-temporal structure is proposed and developed for the analysis of non-stationary nonlinear dynamics of the multimode superradiant lasers with a low-Q cavity and a strong inhomogeneous broadening of lasing transition in an active medium. It is shown that the approach makes it possible to analyze a number of complicated dynamical phenomena in an ensemble of the strongly interacting centers which constitute the active medium and are exposed to CW pumping.

1. Introduction

A non-stationary lasing under CW pumping is a typical dynamical regime which takes place well above a lasing threshold. This regime, as a rule, shows the multimode oscillations which caused by nonlinearity of an active medium, but also may be originated from and complicated by various additional elements inserted into a laser, e.g., by nonlinear absorbers, optical delay feedback, etc. [1-4]. A multimode lasing may exhibit highly non-trivial and even chaotic oscillations which are used in an optical information processing and a wideband spectroscopy. Usually, however, such oscillations are caused by an interaction of cavity modes which are quasi-stationary (weakly modulated) modes and have well-defined spatial structures dictated by an amplification in active medium and by the cavity features, e.g., reflections from the facet mirrors or distributed feedback reflections. Under these conditions, a spatial-temporal evolution of a laser field is described by a superposition of the cavity modes with the time-dependent amplitudes and the spatial profiles, which are fixed and known beforehand. For the standard lasers with high-Q cavities, a resulting dynamical spectrum of the field is usually quasi-equidistant over frequency and homogeneous in time. For a one-dimensional model studied in the present paper, the high-Q cavity modes have the field envelops which are almost constant along a path of wave propagation.

A laser dynamics becomes essentially different in the case of lasers with *low-Q (bad) cavities* where a photon lifetime, T_E, is less than a polarization relaxation time (a lifetime of the optical dipole oscillations), T_2, of the individual active centers excited by pumping. For simplicity's sake, we refer to a well-known two-level model of active medium [1, 4-7] and, for definiteness, we consider the case of a strong inhomogeneous broadening of the lasing transition, $2/T_2^* >> 2/T_2$. Actually, a theoretical analysis of the spatial-temporal dynamics of the field and its spectral and correlation features in such

lasers, known as the superradiant lasers, cannot be based on the above-mentioned standard decomposition on neither 'cold' no 'hot' modes which are defined, respectively, by a cavity without or with taking into account the active medium (under the condition of a steady-state homogeneous population inversion of the lasing energy levels). The point is that the polarization of active centers in the superradiant lasers does not follow adiabatically a value of the local electric field and plays a part of an independent dynamical variable. The field itself flows out of a cavity rapidly and changes in time and space strongly. These effects result in a complicated spatial-temporal dynamics of the population inversion and, hence, lead to an efficient non-adiabatic coupling of cold and/or hot modes what makes those modes useless for the interpretation of collective emission phenomena, even in the case of a steady time-dependent lasing under CW pumping.

A progress in modern technologies, especially in the field of semiconductor heterostructures, leaves no doubts about near fabrication of the dense (in space and spectrum) ensembles of active centers needed for such dynamically rich lasing in the low-Q cavities under CW pumping. (In the case of a pulsed pumping, this kind of a single-burst radiative cooperative phenomenon, known as a collective spontaneous emission, or superfluorescence, has been observed and verified in a number of active-center ensembles, e.g., the ensembles of quantum dots, impurity centers, excitons, and free electrons and holes in quantum wells placed in a quantizing magnetic field [7-15].) Among various regimes, the superradiant lasing includes, first of all, a generation of a sequence of the coherent bunches of pulses of collective spontaneous emission (Dicke superradiance) which is possible at a high rate of pumping, i.e., at a short enough time of incoherent relaxation and creation of inversion of the lasing energy levels of active centers, T_1. The related dynamics of inversion may also provide the conditions for a partial self-locking of the quasi-stationary laser modes which would result in another sequence of pulses with a repetition rate defined by the cavity round-trip time. The expected pulse durations in both sequences lie in the picosecond and/or subpicosecond timescale that gives good prospects for the superradiant-lasing applications in the optical information technologies and the diagnostic techniques for fundamental physics of many-particle systems.

In order to understand the time-dependent space-inhomogeneous configurations of a lasing field in various steady-superradiant regimes and to interpret them properly, we suggest to use a well-known approach of empirical orthogonal functions (EOFs) which is based on a method of the main components [16] and have been widely employed in the analysis of observed space-distributed time series [17-19], including the correlation analysis of data [16, 20]. For the laser problem under consideration, this approach should be generalized and then may be called as an approach of *Space-Time Empirical Modes* (STEMs). The definition and applications of the newly suggested modes are illustrated below on the basis of a numerical solution to the integral-differential Maxwell-Bloch equations for a 1D model of a cavity and an active medium with strong inhomogeneous broadening of a spectral line, $2/T_2^* >> 2/T_2$. Namely, we consider a low-Q hybrid Fabry-Perot cavity with a distribute feedback (DFB) of the counter-propagating waves, where a generation of the superradiant pulses may be accompanied by a partial self-locking of the longitudinal modes without use of any additional technique of mode locking [21, 22].

2. Model of a superradiant laser

According to a preliminary qualitative analysis of dynamics of a superradiant laser with high spatial and spectral density of active centers [23, 24], an output radiation under CW pumping consists, as a rule, of one or several quasi-chaotic sequences of ultrashort powerful pulses and cannot be described as a superposition of any hot modes calculated under the condition of a given homogeneous inversion of a lasing transition in active medium. For a hybrid DFB – Fabry-Perot cavity, a hot mode contains two symmetric counter-propagating waves, each being a sum of two inhomogeneous spatial harmonics with the close wave numbers slightly shifted from the Bragg (DFB) resonance. The hot-mode consideration is sufficient only for the analysis of a quasi-stationary generation regimes with relatively weak and long-term modulation of the mode amplitudes or for the evaluation of a lasing threshold as a

condition of the hot-mode instability [1, 5-7, 22], $\nu_c^2 T_2^* T_E > 1$, where $\nu_c = \sqrt{2\pi d^2 N_0 \omega_{21} / \hbar\bar{\varepsilon}}$ is a so-called cooperative frequency of an ensemble of active centers with a density N_0, d a dipole moment of an active center at the lasing-transition frequency ω_{21}, $\bar{\varepsilon}$ an average dielectric permittivity of an active medium. In our case of the strong inhomogeneous broadening of spectral line, when a parameter $\Delta_0 = \left(\nu_c T_2^*\right)^{-1}$ is large, $\Delta_0 >> 1$, the lasing threshold is defined by a so-called active cooperative frequency [15, 22, 23]: $\bar{\nu}_c \equiv \nu_c / \Delta_0 > 1/T_E$.

In the considered 1D two-level laser model, the dynamics of the field inside a cavity,

$$\mathrm{E}=\mathrm{Re}\left[\left(\tilde{a}_+(z,t)e^{ik_0 z} + \tilde{a}_-(z,t)e^{-ik_0 z}\right)e^{-i\omega_0 t}\right], \tag{1}$$

may be described by the standard semiclassical Maxwell-Bloch equations [1, 4-7, 22] for the dimensionless complex amplitudes of the counter-propagating waves, $a_\pm = \tilde{a}_\pm \bar{\varepsilon} / (2\pi d N_0)$, complex spectral density of the polarization of an active medium, $p_\pm = P_\pm / (dN_0 f(\Delta))$, and related two components of the inversion of energy levels, namely, a slowly varying in space (real) component, $n(\Delta)$, and a half-wavelength modulated (complex) one, $n_z(\Delta)$, originating from the self-consistent beating of the counter-propagating waves. A similar half-wavelength modulated component of the polarization is ignored for simplicity's sake as it plays a minor role under the condition of the strong inhomogeneous broadening of the laser transition. Using slowly varying dimensionless amplitudes, $a_\pm(\varsigma,\tau)$, and taking into account the Bragg coupling of counter-propagating waves due to the spatial modulation of a host dielectric permittivity, $\varepsilon = \bar{\varepsilon}\,\mathrm{Re}[1 + 4\beta\sqrt{I}\exp(2i\varsigma)]$, one can write down the Maxwell equations in a following form

$$\left[\frac{\partial}{\partial\tau} \pm \frac{\partial}{\partial\varsigma}\right] a_\pm = i\beta a_\mp + \frac{i}{\sqrt{I}}\int_{-\infty}^{\infty} p_\pm(\Delta) f(\Delta) d\Delta, \tag{2}$$

where $\Delta = (\omega - \omega_0)/\nu_c$ is a normalized frequency shift from a frequency of the Bragg resonance ω_0; a parameter $I = \nu_c^2 / \omega_{21}^2$ is small, $I << 1$; $\omega_{21} \approx \omega_0$ is a central frequency of the spectral line of the active medium, which is assumed to have the inhomogeneous broadening of a Lorentz type (symmetric with respect to the Bragg resonance), $f(\Delta) = \Delta_0 / \pi(\Delta^2 + \Delta_0^2)$; $\tau = t\nu_c$ and $\varsigma = z\nu_c\sqrt{\bar{\varepsilon}}/c$ are dimensionless time and coordinate; $L = B/B_c$ is a cavity length, B, normalized by means of a cooperative length, $B_c = c/(\nu_c\sqrt{\bar{\varepsilon}})$; $\Gamma_{1,2} = 1/(\nu_c T_{1,2})$ are dimensionless relaxation rates of the inversion and polarization of an active center. The boundary conditions describe reflections of the field at the laser facets with a given complex reflection factor, $\sqrt{R}$ (related to an amplitude a).

3. Traditional empirical modes

The simplest generalization of the known approach of the cold or hot modes [21, 22] is a decomposition of the fields $a_\pm(\varsigma,\tau)$, taken for a dense set of equally spaced grid points along a cavity ($\varsigma_j / \Delta\varsigma = 0,1,2,...,D$, where $\Delta\varsigma = L/D$ is an array pitch which is equal to 0.1 in the following calculations), by means of the time independent *Complex Empirical Orthogonal Functions* (CEOFs), $v_{\pm i}(\varsigma_j)$, which are defined as the normalized eigenvectors of a time-averaged $(D+1)\times(D+1)$ – covariance matrix, $\left\langle a_\pm(\varsigma_j,\tau) a_\pm^*(\varsigma_l,\tau)\right\rangle_\tau$, composed of the gridded data set (the indices j and l

enumerate the rows and columns, respectively) [16, 19, 20]: $a_{\pm}(\varsigma_j,\tau)=\sum_{i=1}^{D+1}Y_{\pm}^{(i)}(\tau)v_{\pm i}(\varsigma_j)$. An averaging is taken over the whole duration of the lasing under consideration (in what follows, it is equal to 16000 units of the dimensionless time τ), and the temporal dynamics is represented by the coefficients $Y_{\pm}^{(i)}$ in that decomposition.

Although the described linear decomposition procedure takes into account only the snap-short correlations of the field at any pair of grid points, it may be sufficient for the analysis of some phenomena in the lasers with low-Q cavities. For instance, if the reflections from the laser facets are not important ($|R|<<1$), the Bragg (DFB) reflections are moderate (so that their characteristic parameter is bounded as $b=\beta L\le\pi$), and the pumping is not too high, the superradiant lasing will contain few hot modes and demonstrate bunches of pulses with short timescales less or of the order of T_E and T_2, but may be quasi-periodic with a long bunch-repetition interval of the order of the time if an inversion repopulation by pumping, T_1, and, in a whole, will be described by even less number (maybe, one) of CEOFs with quasi-periodic amplitudes $Y_{\pm}^{(i)}(\tau)$.

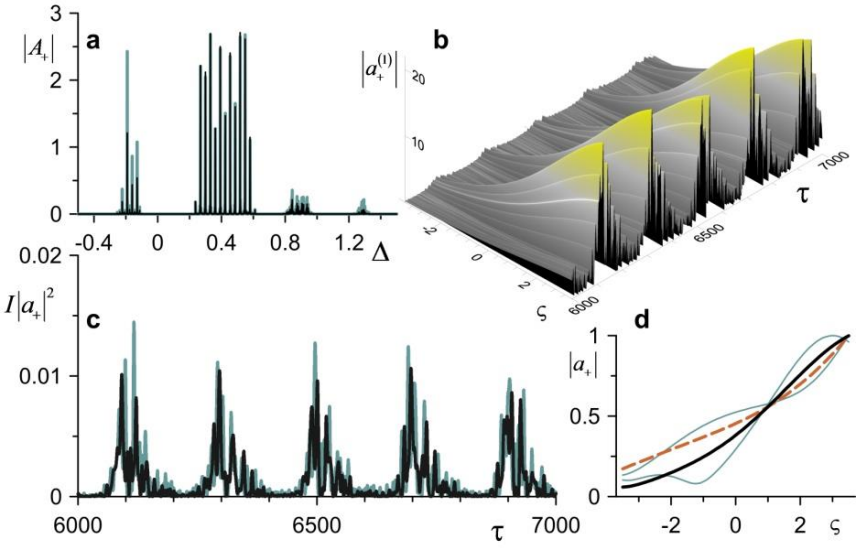

Figure 1. An example of CEOF which describes well the laser emission and fails to depict the field inside a cavity. (a) The spectra of the fields, $|A_+|$, and (c) the corresponding oscillograms of the intensities, $I|a_+|^2$, for a right-propagating wave of the total field (the blue lines) and the field of the main CEOF (the black lines) at a laser facet. (b) A space-time dynamics of the amplitude of this wave $|a_+^{(1)}|$ in the main CEOF. (d) The profiles of the right-propagating wave of the total field (two thin blue lines), the main CEOF (a black line), and the most unstable hot mode (a dashed orange line), which is calculated for the fixed maximum inversion, $n(\Delta)=1$. All profiles are normalized to their maximum values. The laser parameters are: $L=7$, $\sqrt{R}=0.1$, $\Delta_0=4$, $b=0.7$, $\Gamma_1=0.01$, $\Gamma_2=0.03$, $I=25\cdot10^{-6}$.

An example is given in figure 1, where an emission of a laser with the relaxation parameters $T_1\approx3T_2\approx20T_E$ is well described by a single (main) CEOF, $a_{\pm}^{(1)}=Y_{\pm}^{(1)}v_{\pm1}$ (see a plot 1b and the black

lines in the plots 1a, c). In fact, it plays a part of a new hot mode, which can be defined with the use of a time-averaged spatial profile of population inversion. A field profile of this CEOF differs essentially from that of the main unstable hot mode (which is found for a homogeneous inversion of the active medium and shown by the dashed red line in a plot 1d) and makes it possible to characterize an output radiation with a 90% accuracy in energy without use of any STEMs. The description of an outgoing emission may be satisfactory for a large domain of parameters not too far from a lasing threshold. Nevertheless, the field patterns inside a cavity are varied as compared to the main CEOF pattern and need to be analyzed on the basis of the more adequate STEMs (cf. the thin blue lines, which show the field profiles at two moments of time when the maximum superradiant emission is achieved, and the thick black line, which shows the main CEOF, in the plot 1d).

Moreover, if the pumping is rather strong and/or the facet reflections $\sqrt{R}$ are not too weak (as compared to 1 and/or $\tanh(b)$), the several more or less independent sequences of superradiant pulses with different pulse-repetition intervals may be formed due to the oscillations of neighbouring hot modes. Also, a regime of a partial self-locking of the quasi-stationary generating modes with quite uniform frequency spacing at the periphery of the lasing spectrum is possible. It would result in a formation of one more quasi-periodic sequence of pulses with a pulse-repetition interval which is approximately equal or two times less than a cavity round-trip time, i.e., of the order of the value T_E. Bearing all these in mind, one can expect that an essential part of CEOFs will differ from the original cold modes of a cavity or hot modes of a laser, and the whole CEOF approach will be inefficient for the theoretical investigation of the superradiant-laser dynamics.

4. Time-dependent empirical modes

Thus, in many cases a proper description of both the field inside a cavity and the output emission requires a further generalization of the empirical-orthogonal-function approach beyond the CEOF technique. Namely, it is required not only spatial, but also temporal correlation analysis of the gridded data set of complex fields $a_{\pm}(\varsigma,\tau)$, taken at the discrete points along a cavity ($\varsigma_j / \Delta\varsigma = 0,1,2,...,D$, where $\Delta\varsigma = L/D$ is an array pitch) at the discrete moments of time ($\tau_k / \Delta\tau = 0,1,2,...,\mathrm{M}$, where $\Delta\tau = T/M$ is a time step equal to 0.1 in our simulations) within a common time interval $[\tau,\tau+T]$, which is defined by a time scale T under investigation. Systematic investigation of the multi-scale temporal dynamics may even require a use of several series of different generalized empirical modes with different time scales (relevant to various processes), e.g., the averaged periods of generation of the superradiant pulses of various types. In general, a proposed approach follows the techniques of a multidimensional spectral analysis [19, 25, 26] and a compact representation of spatial-temporal data sets [20]. Our approach to the study of the steady or slow varying regimes of lasing originates from the field decompositions (related to different above-mentioned time scales) over the so-called *Space-Time Complex Empirical Orthogonal Functions* (STCEOFs). According to a definition given below, STCEOFs are normalized eigenvectors of the above-mentioned time-averaged extended covariance matrix of a given gridded set of the time-shifted field data capable of taking into account the delayed interparticle interaction, which is owing to the physical processes in the active medium and plays a leading part in many cases. In what follows, depending on a lasing problem and generalizing the standard cold or hot modes, we will introduce also *the Space-Time Empirical Modes (STEMs)* as some individual STCEOFs (including their amplitudes as factors) or some particular steady-state superpositions of several STCEOFs (again, including their amplitudes as factors).

In the following examples, for definiteness, such an approach is performed for a single time scale, $T \approx L$, chosen close to a half cavity round-trip time. The STCEOF construction is carried out separately for each counter-propagating field, $a_{\pm}(\varsigma,\tau)$, represented by the above-mentioned gridded time series. Specifically, for an arbitrary time, τ, we write down a complex column vector, $(a_{\alpha}(\tau))$,

which consists of $(D+1)(M+1)$ elements (enumerated by an index α) grouped as a sequence of the consecutive $M+1$ snap-shorts (maps) of the field (at the moments τ_k), $a(\varsigma_j,\tau_k)$, each given by a $(D+1)-$ column vector (an index j enumerates mesh nodes along a cavity).

The index α may be used in a dual form, $j\mapsto k$, which clearly shows that the consecutive snap-shorts (i.e., $D+1$ values of the field in the grid points $j=0, j=1,\ldots, j=D$) are arranged in a time series according to the growing counts via index $k=0,1,\ldots,\mathrm{M}$: $(a_\alpha(\tau))\equiv(a_{j\mapsto k}(\tau))$, i.e., $(a_\alpha)^T\equiv(a_{0\mapsto 0},a_{1\mapsto 0},\ldots,a_{D\mapsto 0},a_{0\mapsto 1},a_{1\mapsto 1},\ldots,a_{D\mapsto 1},\ldots,a_{0\mapsto M},a_{1\mapsto M},\ldots,a_{D\mapsto M})^T$. What we have to find as the non-stationary STCEOFs are the normalized $(D+1)(M+1)$ – eigenvectors, v_i, of an extended Hermitian covariance matrix, $\langle a_\alpha(\tau)a_\beta^*(\tau)\rangle_\tau$ (α and β enumerate the rows and columns, respectively), which results from the time-averaging of the above-mentioned gridded time series: $(v_i)^T=\left((v_i^{j\mapsto 0})^T,(v_i^{j\mapsto 1})^T,\ldots,(v_i^{j\mapsto M})^T\right)$, where a $(D+1)-$ column vector, $v_i^{j\mapsto k}$, is introduced for the given indices k and i. These eigenvectors v_i contain an important information on a 'fast' dynamics of fields, including the time scales up to the given time scale, T.

Complete dynamics of the fields, including also a 'slow' one with the time scales greater than T, may be seen from a full decomposition of each counter-propagating wave by means of the STCEOF basis and two types of the following expansion functions of time, i.e., the time-dependent complex amplitudes, $Y^{(i)}(\tau)$ and $Z^{(i)}(\tau)=(a(\tau)v_i^*)\equiv\sum_{\alpha=1}^{(D+1)(M+1)}a_\alpha(\tau)\cdot v_i^{*\alpha}$ (for details of a decomposition algorithm, see [25]):

$$a(\varsigma_j,\tau)\equiv\sum_{i=1}^{(D+1)(M+1)}Y^{(i)}(\tau)a^{(i)}(\varsigma_j,\tau)=\sum_{i=1}^{(D+1)(M+1)}\frac{1}{M+1}\sum_{k=0}^{M}Z^{(i)}(\tau-\tau_k)v_i^{j\mapsto k},\qquad(3)$$

where $\tau\geq T$. Here $Y^{(i)}(\tau)$ are the complex amplitudes of the normalized spatial profiles of STCEOFs, $a^{(i)}(\varsigma_j,\tau)$, which are defined by the above time-averaging of a projection of the gridded time series onto the eigenvectors v_i within the time interval T. The terms in the above decomposition of field over the STCEOF basis, $a^{(i)}(\varsigma_j,\tau)$, like in the similar decomposition over the CEOF basis, $v_{\pm i}(\varsigma_j)$, are arranged according to the decreasing order of eigenvalues corresponding to the eigenvectors v_i, since each eigenvalue of an extended covariance matrix is proportional to a relative power of a given STCEOF with respect to a power of the complete laser field. The time scales of these STCEOFs (including their complex amplitudes), $Y^{(i)}(\tau)a^{(i)}(\varsigma_j,\tau)$, are well defined, different and, as a rule, become shorter and shorter for higher numbers *i*, so that the first STCEOFs are responsible for slower dynamics than subsequent ones. We expect that, to pick out qualitatively the main features of the field dynamics in a superradiant laser, it is sufficient to consider several first STCEOFs, which contain, say, 90% or 99 % fraction of the power of laser field.

A field at a laser facet, for instance, at the point $\varsigma=0$, is equal to the same superposition of all STCEOFs (if the reflection factor, $\sqrt{R}$, is taking into account), so that each STCEOF contribution is defined by a product of the time-dependent complex amplitude, $Y^{(i)}(\tau)$, and the known function of time, $a_-^{(i)}(\varsigma=0,\tau)$. For an opposite laser facet, a field of the counter-propagating wave at the point $\varsigma=L$ consists of the sum, $\sum_{i=1}^{(D+1)(M+1)}Y_+^{(i)}(\tau)a_+^{(i)}(\varsigma=L,\tau)$, of all similar STCEOFs, $a_+^{(i)}(\varsigma=L,\tau)$.

5. Examples of the space-time empirical modes

Figures 2 and 3 show an example of a quasi-chaotic emission of a sequence of superradiant pulses originated from a cooperative dynamics of the several different spectral subensembles of active

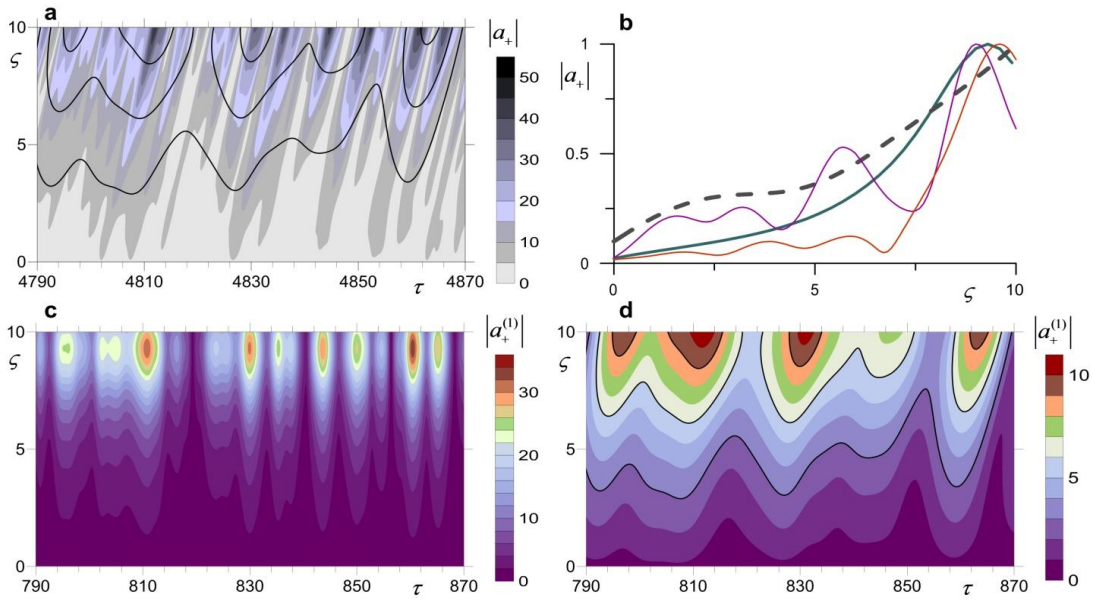

Figure 2. A spatial-temporal structure of the contribution of the right-propagating wave, $|a_+|$, to (a) the total field, (c) the field of the main CEOF, and (d) the field of the first STCEOF defined with a use of a time scale $T = 12.5$. (b) The typical profiles of the right-propagating wave within the total field (two thin colour lines), the main CEOF (a blue line), and the most unstable hot mode (a dashed black line) calculated for the fixed maximum inversion, $n(\Delta) = 1$. All profiles are normalized to their maximum values. The laser parameters are: $L = 10$, $\sqrt{R} = 0.1e^{i\pi/2}$, $\Delta_0 = 4$, $b = 1$, $\Gamma_1 = 0.01$, $\Gamma_2 = 0.02$, $I = 25 \cdot 10^{-6}$. The contours of a plot (d) are put onto a plot (a) in order to compare the dynamics of the total field ($|a_+|$) and the field of the first STCEOF ($|a_+^{(1)}|$).

centers, or, in other words, caused by the instabilities of several different hot modes of the laser. According to figure 2, a travelling-wave nature of the total field is well described by the first STCEOF which contributes about a quarter of the total power. A field of the main CEOF, which contributes a bit higher than a half of the total power, has nothing to do with this travelling-wave phenomenon and, in fact, contains an information on some averaged field profile in the cavity only. It is useful to combine two first STCEOFs in one STEM. Then, the latter contains a bit less than a half of the total field power, covers a well-defined range of spectrum (see figure 3b), and yields a precise, complete description of the sequence of the superradiant pulses emitted by a subensemble of the active centers which have spectral localization in a vicinity of the photonic bandgap (owing to the Bragg DFB) and are closely related to the most unstable two hot modes situated at the bandgap edges. A typical duration of these superradiant pulses is of the order of the cavity lifetime, $T_E \approx 8$, and much less than the relaxation time of polarization, $T_2 = 50$. Similarly, the next STCEOFs make it possible to describe other sequences of superradiant pulses emitted by the neighbouring spectral subensembles of active centers.

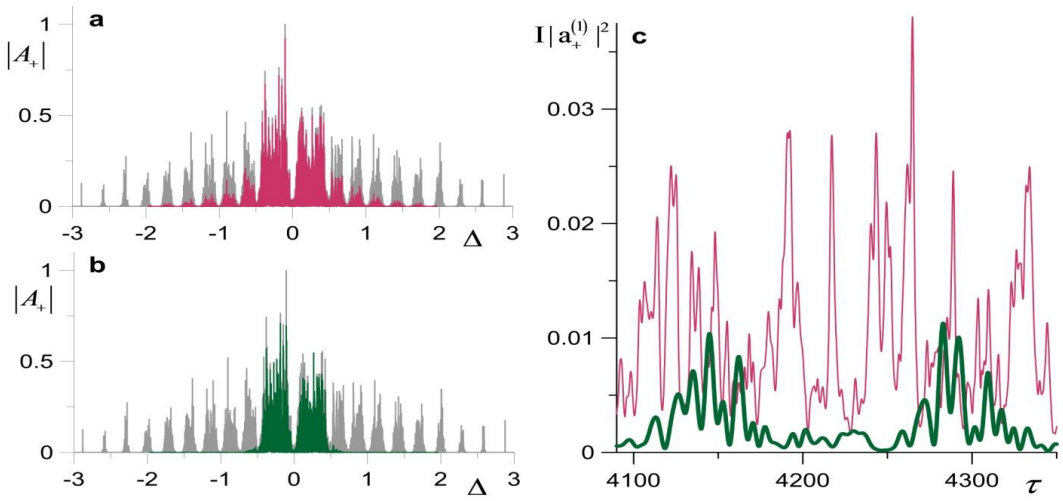

Figure 3. The spectra of the total field (the grey lines on the plots (a) and (b)), the field of the main CEOF (a red line on a plot (a)), and the main STEM formed by a superposition of the first two STCEOFs (a green line on a plot (b)). A comparison of the oscillograms of an intensity, $I|a_+^{(1)}|^2$, of the field of the main CEOF (a red line on a plot (c)) and the main STEM (a green line on a plot (c)) is also shown. The laser parameters are: $L=10,\ \sqrt{R}=0.1e^{i\pi/2},\ \Delta_0=4,\ b=1,\ \Gamma_1=0.01,\ \Gamma_2=0.02,\ I=25\cdot10^{-6}$.

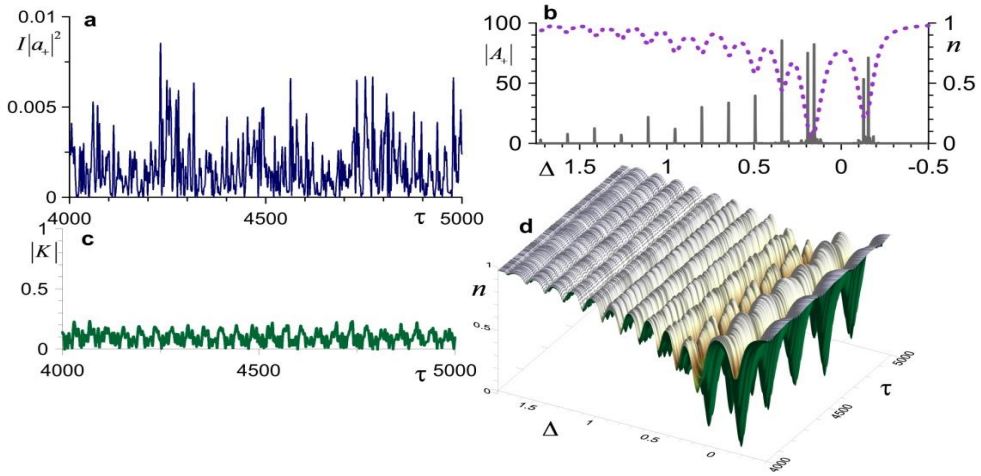

Figure 4. (a) An oscillogram of the intensity, $I|a_+|^2$, of a right-propagating wave. (b) A spectral distribution of the population inversion, $n(\Delta)$, (at a moment of time when a superradiant pulse is emitted) and a spectrum of the field, $|A_+|$, at a laser facet. (c) A correlation function, $|K|=\left|\int_{-\bar{T}/2}^{\bar{T}/2} a(t)a^*(t+\tau)dt\right| \Big/ \int_{-\bar{T}/2}^{\bar{T}/2} |a(t)|^2\,dt$, of the field at a laser facet for a time-averaging interval much greater than a typical interval between the bunches of superradiant pulses ($\bar{T}\approx1000$). (d) A dynamical spectrum of the population inversion of the lasing transition. The laser parameters are: $L=20,\ \sqrt{R}=0.1,\ \Delta_0=13,\ b=\sqrt{3},\ \Gamma_1=0.01,\ \Gamma_2=0.03,\ I=2.3\cdot10^{-6}$.

A STEM-based analysis provides a deep qualitative insight into the straightforward numerical solution to the integral-differential equations of a superradiant-laser dynamics [21-24, 27-30] and

makes it possible to pick out the important features of the above-mentioned regimes of oscillations under CW pumping. In a rest part of the paper, we will consider one such regime which takes place

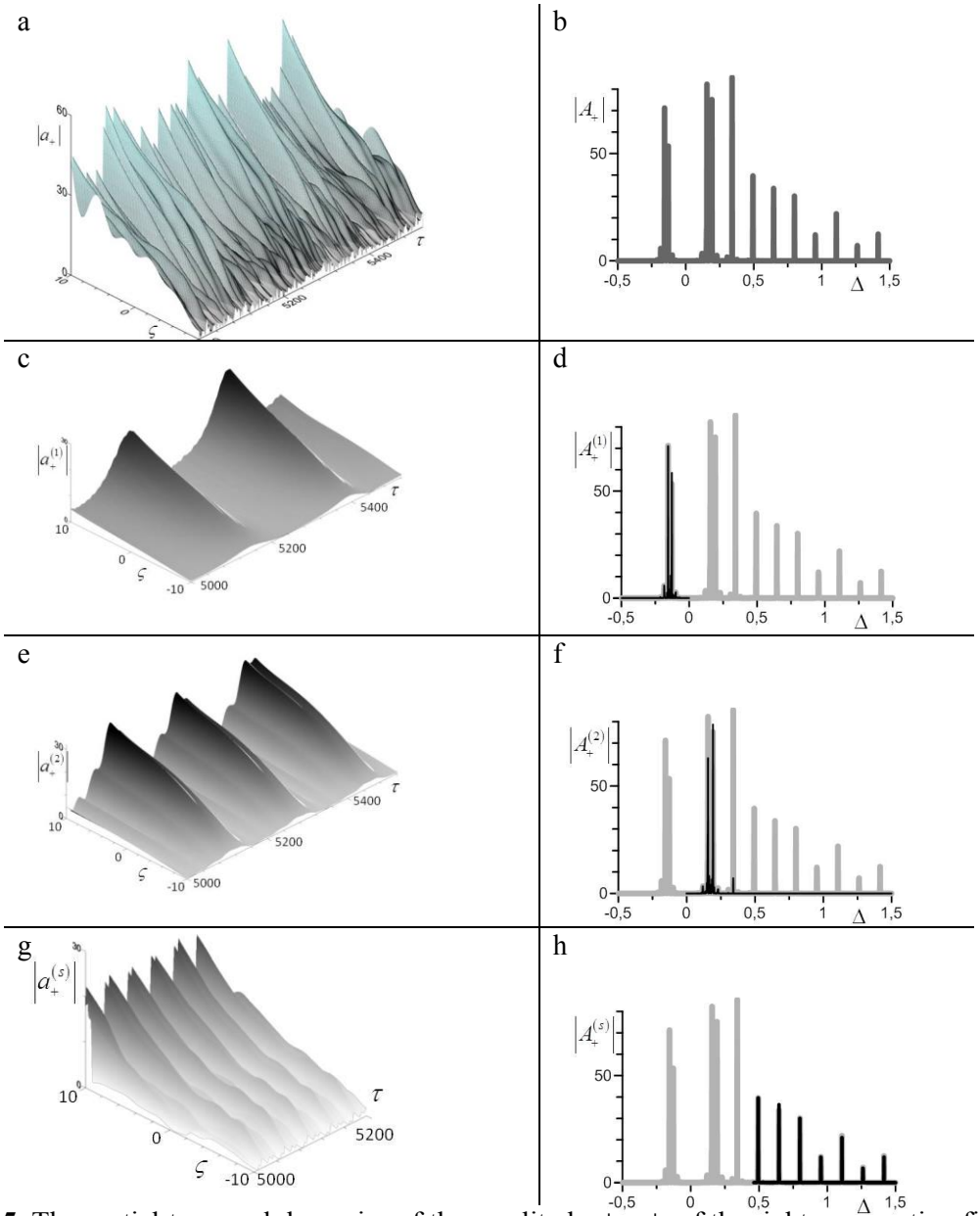

Figure 5. The spatial-temporal dynamics of the amplitude, $|a_+|$, of the right-propagating field and the spectrum of this field, $|A_+|$, at a laser facet in the case of the multimode oscillations under CW pumping. (a), (b) The total field and its spectrum. (c), (d) The field and spectrum of the first STCEOF which describes one independent superradiant mode (shown by black on a grey background of the total spectrum). (e), (f) The field and spectrum of the second STCEOF which describes another superradiant mode and demonstrates a nonlinear interaction with the quasi-stationary lasing modes from a right-hand side of the total spectrum. (g), (h) The field and spectrum of a combined STEM which is defined as a superposition of seven STCEOFs, from 4^{th} to 10^{th} ones (again shown by black), and represents the main part of a pulse formed due to the self-mode-locking effect. All STCEOFs are calculated with a use of a time scale $T = 20$. The laser parameters are: $L = 20$, $\sqrt{R} = 0.1$, $\Delta_0 = 13$, $b = \sqrt{3}$, $\Gamma_1 = 0.01$, $\Gamma_2 = 0.03$, $I = 2.3 \cdot 10^{-6}$.

not far from a superradiant threshold in the case when a spectrum of the excited hot modes of a low-Q combined DFB – Fabry-Perot cavity is enriched due to a mutual action of the weak reflections at the laser facets and a nonlinear coupling between the Fourier components of the superradiant field outside the photonic band gap and the spectrally remote quasi-stationary laser modes. Then, in general, the laser radiation has a form of a nonlinear superposition of a quasi-periodic or quasi-chaotic sequence of the ultrashort powerful superradiant pulses (figure 4a) and a quasi-periodic (more regular) sequence of the comparable pulses formed by the quasi-stationary self-locked modes of the Fabry-Perot cavity with an equidistant spectrum (figure 4b). The latter are locked, that is obey certain phase relations, due to an effect of saturation of a pulse absorption which takes place in the presence of the deep spectral holes of population inversion (figure 4b, a dashed line, and figure 4d) as it may tend to zero or even become negative during the action of the superradiant pulses.

In the above example, a degree of correlation of the quasi-chaotic radiation at a laser facet is not high (less than 25% in figure 4c) because there are continuous beatings between some pulses of more or less independent origin which are comparable in power and have different time scales. Mainly, these are the partially formed superradiant pulses which are generated in the two spectral channels at the edges of the photonic band gap and have a duration of the order of the relaxation time of polarization, $T_2 \approx 1.5T_E \approx 34$. A repetition interval is on the order of time it takes the pumping to restore a high level of the population inversion, $T_1 = 100$. These pulses interfere also with the self-mode-locked pulse which is travelling (and distributed) around a cavity and responsible for a formation of a sequence of more frequent emission pulses with an average repetition interval $T \approx L = 20$ and even shorter duration less than the above-mentioned relaxation times.

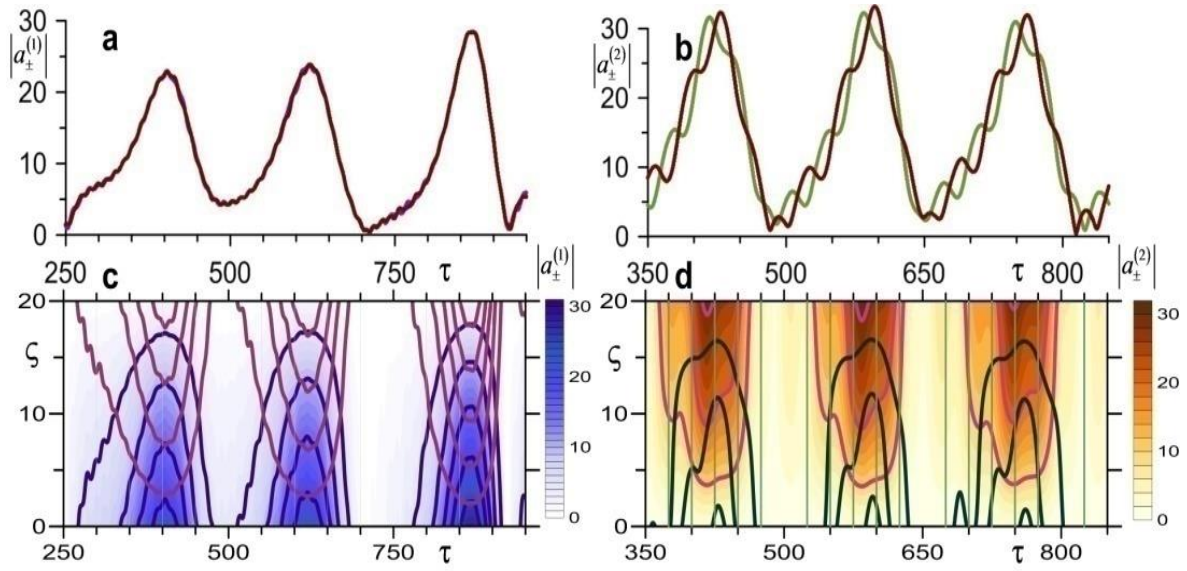

Figure 6. (a), (b) The oscillograms of the amplitudes of the counter-propagating waves, $|a_\pm|$, (at the opposite laser facets) of the first and second superradiant STEMs defined as the first and second STCEOFs, respectively. (c), (d) The spatial-temporal dynamics of the amplitudes of these waves, $|a_\pm(\varsigma,\tau)|$. The laser parameters are: $L = 20$, $\sqrt{R} = 0.1$, $\Delta_0 = 13$, $b = \sqrt{3}$, $\Gamma_1 = 0.01$, $\Gamma_2 = 0.03$, $I = 2.3 \cdot 10^{-6}$.

The unique simultaneous generation of the two pulse sequences comparable in power and different in the spectral and temporal scales (both may differ by many times) is worth to analyze in detail by means of the universal STCEOF basis (figure 5). Note that a straightforward modeling of the

Maxwell-Bloch equations does not allow one to separate the space-time structures of individual modes under consideration, and an actual experiment has nothing to say on this account as well.

According to figure 5, the discussed complicated quasi-chaotic oscillations (shown in figures 4a and 5a), in fact, result from a combination of three quite regular dynamics separated in spectrum and described by a pair of the superradiant STEMs, which correspond to the 1st and 2nd STCEOFs, respectively, (figure 5c, e, figure 6) and an additional combined STEM, which is formed by a group of the 4th to 10th STCEOFs (figure 5g, figure 7) and represents the main part of the self-mode-locked pulse. An interaction of the latter with the two superradiant modes is mediated by third STCEOF which is not shown in the left column of figure 5.

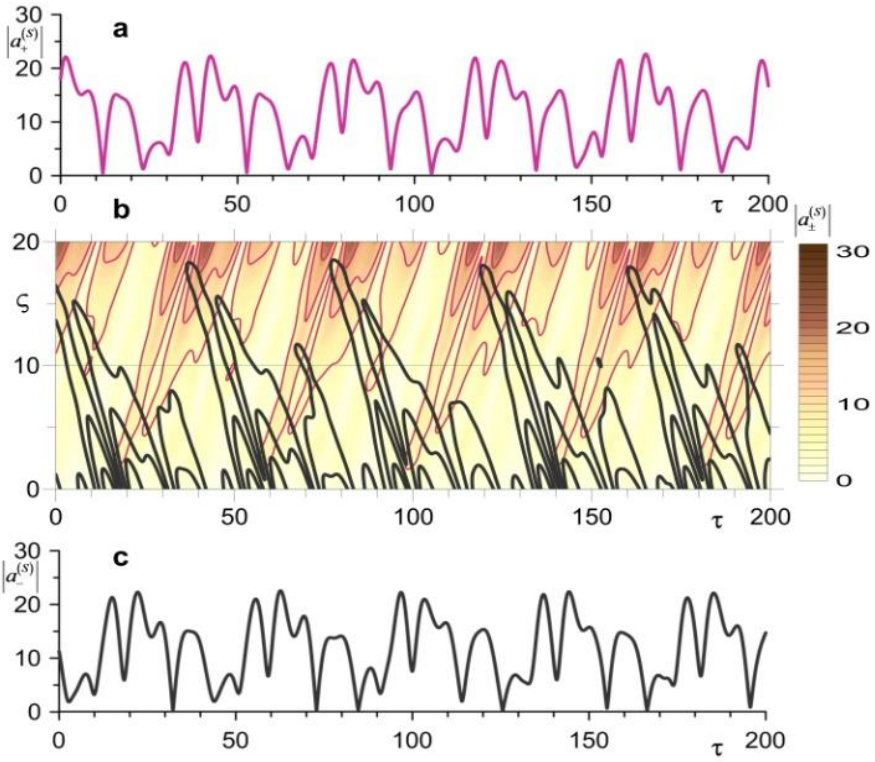

Figure 7. The oscillograms of the amplitudes of the counter-propagating waves, $|a_{\pm}^{(S)}|$, of the combined STEM (see a right-hand side of the spectrum in Fig. 5h) related to the main part of the round-travelling pulse which is formed by the self-locked hot modes and produces an output radiation from the right (a, a red line) and left (c, a black line) laser facets. (b) The spatial-temporal dynamics of the amplitudes of the right-propagating (the red contours) and left-propagating (the black contours) waves, $|a_{\pm}^{(S)}(\varsigma,\tau)|$, of the same STEM. The laser parameters are: $L=20,\ \sqrt{R}=0.1,\ \Delta_0=13,\ b=\sqrt{3},\ \Gamma_1=0.01,\ \Gamma_2=0.03,\ I=2.3\cdot10^{-6}$.

The superradiant STEMs, each of them consists of two counter-propagating waves with a smooth (within a cavity length scale) non-stationary spatial structure, are emitted simultaneously from the opposite laser facets (see two pairs of curves, $a^{(1)}(\tau)$ and $a^{(2)}(\tau)$, in figure 6a, b and, hence, have a standing-wave (mode) character (a shallow ripple in figure 6b and a weak phasing-out of the amplitude oscillations in figure 6d are not important statistically). The time scales of the first two

STEMs differ essentially ($\tau_1 = 250$ and $\tau_2 = 150$, respectively). The third (combined) STEM, $a^{(S)}(\tau)$, consists of the fields of seven STCEOFs, each of them contributes to a spectrum of two or three different hot modes of the laser. This STEM describes a spatial-temporal structure of the self-mode-locked pulses which are periodic in time and extend over the whole cavity in such a way that they repeat themselves after every successive reflection at each laser facet. The counter-propagating waves, present in these pulses and shown in figure 7b by the red and black contours, re-emit each other continuously when moving across the Bragg periodic lattice of the dielectric permittivity in the DFB – Fabry-Perot cavity. It is the unique combine STEM that clarifies the complicated spatial-temporal structure of the round-travelling self-mode-locked pulses.

6. Conclusions

The presented examples of the space-time empirical modes (STEMs) prove that these modes are useful for the analysis of complicated features of a strongly non-stationary field which are typical for the superradiant lasing in the low-Q cavity. Thus, the suggested STEM approach is an efficient tool in the dynamical theory and interpretation of various regimes of the superradiant lasers as well as in the development of their applications in the optical information processing, the wideband dynamical spectroscopy, and the diagnostics of the many-particle processes in condensed active media.

Acknowledgements

The work was partially supported by the Russian Foundation for Basic Research (a grant # 16-02-00714) and the Program of Fundamental Research of the Physical Science Brunch of the Russian Academy of Sciences (a project # III.7 “Fundamentals and experimental development of the perspective semiconductor lasers for the industrial and technological purposes”) and the Competitiveness Program of National Research Nuclear University “MEPhI”. One of the authors (V.V. Kocharovsky) is very grateful for the nice hospitality of MEPhI during his visit supported by the mentioned Program.

References

[1] Khanin Ya. L. 2006 *Fundamentals of Laser Dynamics* (Cambridge: Cambridge International Science Publishing)
[2] Arecchi F T and Harrison R G 2011 *Instabilities and Chaos in Quantum Optics* (London: Springer Verlag)
[3] Ohtsubo J 2013 *Semiconductor Lasers: Stability, Instability and Chaos* (Series: Springer Series in Optical Sciences vol. 111)
[4] Roldan E et al 2005 Trends in Spatiotemporal Dynamics in Laser. Instabilities, Polarization Dynamics, and Spatial Structures (Trivandrum: Research Signpost) (Preprint http://www.arXiv: physics/0412071V1)
[5] Belyanin A, Kocharovsky V, Kocharovsky Vl 1997 Collective QED processes of electron-hole recombination and electron-positron annihilation in a strong magnetic field *Quantum and Semiclassical Optics* **9** 1
[6] Zheleznyakov V, Kocharovskii V, Kocharovskii Vl 1989 Polarization waves and superradiance in active media *Sov. Phys. Usp.* **32** 835
[7] Golubyatnikova E, Kocharovsky V, Kocharovsky Vl 1997 Mode Instability and Nonlinear Superradiance Phenomena in Open Fabry-Perot Cavity *International Journal of Computers and Mathematics with Applications* **34** 773
[8] Qiao P et al 2013 Theory and experiment of submonolayer QD metal-cavity surface-emitting microlasers *Optics Express* **21** 30336
[9] Ding C et al 2012 Observation of In-related collective spontaneous emission (superfluorescence) in Cd0.8Zn0.2Te:In crystal *Appl. Phys. Lett.* **101** 091115
[10] Dai D and Monkman A 2011 Observation of superfluorescence from a quantum ensemble of coherent excitons in a ZnTe crystal: Evidence for spontaneous Bose-Einstein condensation

of excitons *Phys. Rev. B* **84** 115206
[11] Germann T et al 2008 High-power semiconductor disk laser based on InAs/GaAs submonolayer quantum dots *Appl. Phys. Lett.* **92** 101123
[12] Scheibner M et al 2007 Superradiance of quantum dots *Nature Physics* **3** 106
[13] Kim J et al 2013 Fermi-edge superfluorescence from a quantum-degenerate electron-hole gas *Scientific Rep*. **3** 3283
[14] Jho Y et al 2010 Cooperative recombination of electron-hole pairs in semiconductor quantum wells under quantizing magnetic fields *Phys. Rev.* B **81** 155314
[15] Kalinin P et al 2012 On the problem of lasing in traps for the Bose condensation of dipolar excitons *Semiconductors* **46** 1351
[16] Jollife I 1986 Principal Component Analysis (Springer)
[17] Hannachi A, Jolliffe I and Stephenson D 2007 Empirical orthogonal functions and related techniques in atmospheric science: A review *Int. J. Climatol*. **27** 1119
[18] Monahan A et al 2009 Empirical Orthogonal Functions: The Medium is the Message *Journal of Climate* **22** 6501
[19] Navarra A and Simoncini V 2010 *A Guide to Empirical Orthogonal Functions for Climate Data Analysis* (Springer Science+Business Media B.V.)
[20] Mukhin D et al 2015 Predicting critical transitions in ENSO models II: Spatially dependent models *Journal of Climate* **28** 1962
[21] Kocharovsky Vl et al 2013 Dynamics of the class D lasers based on the Bose-Einstein condensates, the submonolayer quantum dots and other exotic active media *Nonlinear waves'2012* (Nizhny Novgorod: IAP RAS) pp 398-428 (in Russian)
[22] Kocharovsky Vl et al 2015 Superradiant Lasing and Collective Dynamics of Active Centers with Polarization Lifetime Exceeding Photon Lifetime *Advanced Lasers: Laser Physics and Technology for Applied and Fundamental Science* ed. O Shulika (Series: Springer Series in Optical Sciences. V. 193) chapter 4 pp 49-69.
[23] Kocharovsky Vl et al 2010 Perspectives of creation of a superradiant heterolaser *Proc. II Symp. on coherent optical radiation of semiconductor materials and structure* (Moskow: Lebedev Institute of Physics, RAS) p 68 (*in Russian*)
[24] Kalinin P et al 2012 Features and coherence of pulses generated by the superradiant lasers based on the multilayered Bragg heterostructure with submonolayer quantum dots under the conditions of self-mode-locking of longitudinal modes *Proc. III Symp. on coherent optical radiation of semiconductor materials and structure* (Moskow: Lebedev Institute of Physics, RAS) p 71 (*in Russian*)
[25] Ghil M et al 2002 Advanced spectral methods for climatic time series *Rev. Geophys*. **40** 1
[26] Plaut G and Vautard R 1994 Spells of oscillations and weather regimes in the low-frequency dynamics of the Northern Hemisphere *J. Atmos. Sci.* **51** 210
[27] Kocharovskaya E et al 2015 The Dynamical Spectra of the Superradiant Heterolasers: Spatial-Temporal-Dependent Mode Technique Versus Cold or Hot Mode Techniques *Tech. Digest Int. Workshop "Nonlinear Photonics: Theory, Materials, Applications" NPh-15* pp 46-7
[28] Loskutov E et al 2015 Spatial-temporal empirical modes as an instrument of studying superradiant laser dynamics *Thesis Int. Workshop "DyNeMo-Clim"* p 34
[29] Kocharovsky Vl and Kocharovsky V 2016 Progress and perspectives of the superradiant lasers *Proc. XX Int. Symposium "Nanophysics and Nanoelectronics"* vol 2 p 632 (*in Russian*)
[30] Kocharovskaya E et al 2015 Superradiant semiconductor distributed-feedback lasers. An analysis of dependence of a laser dynamics on a relation of between the relaxation times of a field and a polarization of active medium *Proc. XX Int. Symposium "Nanophysics and Nanoelectronics"* vol 2 p 630 (*in Russian*)